Journal of Molecular Structure 1206 (2020) 127663

Contents lists available at ScienceDirect

Journal of Molecular Structure

journal homepage: http://www.elsevier.com/locate/molstruc

Investigation of electrical conductance properties, non-covalent interactions and TDDFT calculation of a newly synthesized copper(II) metal complex

Samit Pramanik [a], Saugata Konar [b, **], Koushik Chakraborty [c], Tanusri Pal [d], Sourav Das [e], Sudipta Chatterjee [f], Malay Dolai [g], Sudipta Pathak [h, *]

[a] Department of Chemistry, Jadavpur University, Jadavpur, Kolkata, 700032, India
[b] Department of Chemistry, The Bhawanipur Education Society College, Kolkata, 700020, India
[c] Department of Physics & Technophysics, Vidyasagar University, Midnapore, 721102, West Bengal, India
[d] Department of Physics, Midnapore College, Midnapore, 721101, West Bengal, India
[e] Department of Chemistry, Institute of Infrastructure, Technology, Research, and Management (IITRAM), Ahmedabad, 380026, India
[f] Department of Chemistry, Serampore College, Serampore, Hooghly, 712201, India
[g] Department of Chemistry, Prabhat Kumar College, PurbaMedinipur, 721404, India
[h] Department of Chemistry, Haldia Govt. College, Haldia, PurbaMedinipur, 721657, India

ARTICLE INFO

Article history:
Received 24 November 2019
Received in revised form
24 December 2019
Accepted 26 December 2019
Available online 3 January 2020

Keywords:
Copper(II) complex
X-ray crystal structure
Non-covalent interactions
Electrical conductivity
TDDFT calculation

ABSTRACT

[Cu(pydc)(apy)]·3H_2O (**1**) ($pydcH_2$ = pyridine-2,6-dicarboxylic acid; apy = 2- aminopyridine) has been synthesized and characterized by elemental analysis, IR spectroscopy and single crystal X-ray diffraction techniques. Crystallographic analysis tells that the complex **1** has distorted square pyramid geometry with $pydcH_2$ coordinated as a tridentate ligand to each metal ion through two oxygen atoms of each carboxylate group and the nitrogen atom of the pyridine moiety. Three non-coordinated water molecules are present in the asymmetric unit and all are involved in constructing a $(H_2O)_6$ cluster with chair conformation like cyclohexane. Interestingly, The average O···O distance of 2.759 Å in water hexamer of Complex **1** is closer to the respective distance of ice (2.76 Å for ice I_h at 90 K) than to that of bulk liquid water (2.85 Å). Also, the average O—O—O bond angle of 107.96° is close to the tetrahedral angle in ice I_h form. Apart from water cluster, the aromatic molecules are engaged in several non-covalent interactions like NH … π, lone pair … π, π … π and hydrogen bonds. These types of non-covalent interactions attribute to the supramolecular framework of the studied molecule. The electrical conductivity in terms of current was measured at room temperature before and after annealed of the synthesized complex compound on thin film specimen of order 230 and 240 μA respectively with bias voltage 1 V. In addition, the electronic transitions of **1** were recorded and the electronic distribution of HOMO-LUMO was rationalized theoretically (through time-dependent density functional theory (TDDFT)).

1. Introduction

The field of crystal engineering has vastly studied and demonstrated highlighting metal organic frame work with specific solid-state properties [1]. Early investigation of crystal engineering was mainly focused on the syntheses of coordination compounds but later considerable attention was drawn on supramolecules for their imperative and exceptional topologies. Recent scientists in this field of research are engaged to explore their wide practical utilities in diverse technological and industrial areas, like specific molecular gas adsorption, and capture or storage, [2] heterogeneous catalysis, [3] biomedicine, [4] nanotechnology, [5] photoluminescence, non-linear optics, sensors [6], *etc*. In this context, crystal engineering is interlinking chemistry and crystallography to investigate the self-assembly process, interesting topologies and novel properties of various transition metals based complex compounds. Target oriented synthesis of metal organic framework through a self-assembly process is often not achieved. This is due to sensitive

* Corresponding author.
** Corresponding author.
E-mail addresses: saugata.konar@gmail.com (S. Konar), sudiptachemster@gmail.com (S. Pathak).

https://doi.org/10.1016/j.molstruc.2019.127663
0022-2860/

dependence on the surrounding environmental conditions during synthesis leading to a number of unexpected products from a particular set of building blocks [7]. Then formation of metal organic framework can be explained by multiple non-covalent interactions through sequences of molecular recognition events (hydrogen bonding, anion-π interaction, aromatic ring stacking, *etc*) [8–10]. Approximately, 25% of all crystal structures known so far grown from water form hydrates. Thus the roles and influencing factors of water molecules are yet to be disclosed in a solid-state architecture [11]. Coordination capability and strong hydrogen bonding ability of water molecules are often incorporated into the metal–organic frameworks (MOFs) giving rise to dimers and higher order oligomers [12].

Multicarboxylate and *N*-heterocyclic based ligands are widely employed in several areas like coordination chemistry, medicine, especially HIV investigations, biochemistry, and proton transfer reactions [13,14]. In this context, pyridine-2,6-dicarboxylic acid ($pydcH_2$) is widely used because of its low toxicity. It also shows diversified biological activity being observed in many natural products such as oxidative degradation product of vitamins, alkaloids, coenzymes [15,16].

$PydcH_2$ and complexation compounds of $pydcH_2$ with different metallic ions have also attracted much attention in designing and synthesis of such compounds because of their interesting topologies, promising structural features, enthralling functionalities. These all promote wide practical utility in photoluminescence, molecular adsorption and gas storage, catalysis and magnetism [17–21].

Recently, Mirzaei et al. reported a very analogous dicarboxylic acid precursor of chelidamic acid as an efficient proton donor [22]. Inspiring from these works and as the continuation of our research we have investigated the coordination behavior of pyridine-2,6-dicarboxylic acid ($pydcH_2$) in presence of copper(II) ion and aromatic amine derivative.

Herein, we report the syntheses, structural features, spectroscopic characterization and X-ray crystal structures of a new complex of copper(II) and its electrical conductivity is also studied. Different crystalline architectures are obtained *via* various non-covalent interactions like H-bonding, lone pair … π, NH … π and π … π interactions. To understand the electronic structures of complex **1** DFT (Density Functional Theory) calculations have been carried out and furthermore TDDFT (Time Dependent Density Functional Theory) calculations have been done on the DFT optimized geometries, to interpret the electronic transitions accurately.

2. Experimental methods

2.1. General methods and materials

All the chemicals were of AR grade and obtained from commercial sources (SD Fine Chemicals, India or Aldrich) and used without further purification.

2.2. Physical measurements

IR spectra were recorded in the region 4000–400 cm^{-1} using a Perkin–Elmer model 883 infrared spectrophotometer. Elemental analyses (C, H and N contents) were carried out by a Perkin–Elmer CHN analyzer 2400 at the Indian Association for the Cultivation of Science, Kolkata. Current (I) - Voltage (V) measurement at room temperature were taken before and after annealed by a Keithley 2611A source meter. Lab Tracer 2.0 software was used to collect and analyze the electrical data.

2.3. Synthesis

2.3.1. Synthesis of [Cu(pydc)(apy)]·3H_2O (1)

An aqueous solution of $CuCl_2 \cdot 6H_2O$ (4 mmol, 0.968 g) was added to an aqueous solution of pyridine-2,6-dicarboxylic acid ($pydcH_2$) (4 mmol, 0.668 g) and 2-aminopyridine (apy) (4 mmol, 0.376 g) under stirring at 40 °C for nearly 3 h. Green colored crystals were obtained by slow evaporation of the reaction mixture at room temperature. Elemental analysis: anal. calc. for $C_{12}H_{15}CuN_3O_7$: C, 38.21; H, 3.98; N, 19.10. Found: C, 38.11; H, 3.94; N, 19.19%. IR bands (KBr pellet, cm^{-1}): 3404, 3010, 1645, 1702, 1450, 1323, 745.

2.4. X-ray crystallography study

Selected crystal data for **1** is given in Table 1 and selected metrical parameter of the complex is given in Table 2. For **1** data collections were made using Bruker SMART APEX II CCD area detector equipped with graphite monochromated Mo Kα radiation (λ = 0.71073 Å) source in φ and ω scan mode at 273(2) K. Cell parameters refinement and data reduction were carried out using the Bruker SMART APEX II. Cell parameters refinement and data reduction were carried out using Bruker SMART [23] and Bruker SAINT softwares for all the complexes. The structure of all the complexes were solved by conventional direct methods and refined by full-matrix least square methods using F2 data. SHELXS-97 and SHELXL-97 programs [24] were used for determining structure of the complexes solution and refinement respectively.

2.5. Device fabrication for electrical conductivity measurement

Thin film was fabricated on a pre-cleaned glass substrate for electrical conductivity measurement by simple drop casting method. At the time of drop casting, the glass was placed on a hot plate to evaporate the solvent in which synthesized material was dissolved. Two parallel electrodes of conducting silver paint (Ted Pella) were drawn on the thin film with average separation ~ 5 mm. At the time of measurement, the two parallel probes were connected to Keithley 2611A Source Meter and data was collected by using Lab Tracer acquisition card.

Table 1
Experimental data for crystallographic analysis of complex **1**.

Compound	**1**(CCDC 1531475)
Empirical formula	$C_{12}H_{15}CuN_3O_7$
Formula weight	376.82
Temperature (K)	273(2)
Crystal system	Triclinic
Space group	P-1
Unit cell dimensions	
a (Å)	7.5054(5)
b (Å)	9.7491(6)
c (Å)	11.3065(10)
α (°)	108.637(3)
β (°)	96.497(4)
γ (°)	111.849(2)
Volume ($Å^3$)	701.82(9)
Z	2
$Density_{cal}$ (Mg m^{-3})	1.783
Absorption coefficient (mm^{-1})	1.600
F(000)	386
Independent reflections [R_{int}]	2465 [R(int) = 0.041]
Data/restraints/parameters	2465, 13, 238
Reflections collected	9713
Final R indices [I > 2σ (I)]	R1 = 0.0457, WR2 = 0.1323
Largest difference peak and hole ($eÅ^{-3}$)	−0.89, 0.58

Table 2
Selected bond distances (Å) and angles (°) data for **1**.

Selected Bonds	(Å)	Selected Angles	(°)
Complex 1			
Cu1—O1	2.013(3)	O1—Cu1—O3	160.57(12)
Cu1—O3	1.992(3)	O1—Cu1—N1	99.04(13)
Cu1—N1	1.9337(14)	O1—Cu1—N3	80.49(13)
Cu1—N3	1.906(3)	O1—Cu1—O2_a	81.10(11)
Cu1—O2_a	2.739(4)	O1—Cu1—N2_b	89.36(11)
Cu1—N2_b	2.768(4)	O3—Cu1—N1	100.38(13)
		O3—Cu1—N3	80.11(14)
		O2_a-Cu1-O3	98.26(11)
		O3—Cu1—N2_b	92.34(11)
		N1—Cu1—N3	178.98(15)
		O2_a-Cu1-N1	89.62(13)
		N1—Cu1—N2_b	87.13(13)
		O2_a-Cu1-N3	91.21(13)
		N2_b-Cu1-N3	91.96(14)
		O2_a-Cu1-N2_b	169.31(10)

Translation of Symmetry Code to Equiv.Pos, a = [2656.00] = 1-x,-y,1-z, b = [2666.00] = 1-x,1-y,1-z.

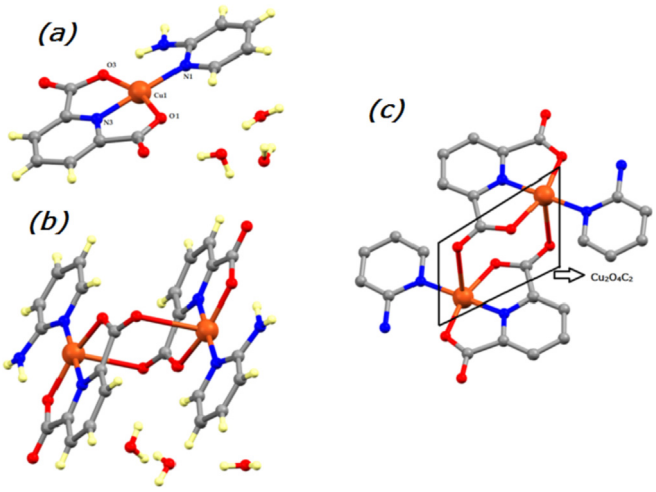

Fig. 1. (a) The asymmetric unit of **1**, (b) The molecular structure of **1**, (c) Motif of eight-membered puckered ring of **1**.

2.6. Computational details

The ground state electronic structure calculation in gas phase of complex **1** has been carried out using DFT [25] method connected with the conductor-like polarizable continuum model (CPCM) [26]. Becke's hybrid function [27] with the Lee-Yang-Parr (LYP) correlation function [28] was used during the study. The absorbance spectral properties in DMF medium was calculated by time-dependent density functional theory (TDDFT) [29] associated with the conductor - like polarizable continuum model. We computed the lowest 40 singlet − singlet transition.

For C, H, N, O, and Cu atoms, we used 6-31 + g as basis set for all the calculations which were performed with the Gaussian 09W software package [30]. Gauss Sum 2.1 program [31] was used to calculate the molecular orbital contributions from groups or atoms.

3. Results and discussion

3.1. Crystal structure description of *1*

Single − crystal X-ray diffraction analysis reveals that complex **1** is neutral, binuclear and crystallizes in a triclinic system in the space group *P*-1 with $Z = 2$. The asymmetric unit of **1** contains one-half of the total molecule, *viz*., [Cu^{II}(pyridine-2,6-dicarboxylate)(2-amino-pyridine)].3H_2O (Fig. 1a). The molecular structure of **1** is represented in Fig. 1b and selected bond lengths and angles of complex **1** are given in Table 2.

Detailed structural analysis shows that the dinuclear complex **1** is assembled by the cumulative coordination action of two fully deprotonated pyridine-2,6-dicarboxylate ligands and two amino pyridine ligands. Deprotonated form of pyridine-2,6-dicarboxylate ligand has five potential coordination sites (four oxygen centers of carboxylate group and one pyridine nitrogen centre) but three have been used for binding to the metal sites in asymmetric unit. On the other hand, only one coordination site in 2-aminopyridine ligand is involved to coordinate the metal centre. Each deprotonated pyridine-2,6-dicarboxylate ligand and 2-aminopyridine ligand hold one Cu^{II} metal centre to forma mononuclear subunit, [Cu^{II}(pyridine-2,6-dicarboxylate)(2-aminopyridine)]. The carboxylate oxygen atoms function as a bridging ligand between the two Cu^{II} centers. Within molecular structure, fully deprotonated pyridine-2,6-dicarboxylate adopts $\eta^1{:}\eta^1{:}\eta^1{:}\eta^1$coordination mode of carboxylate anions and 2-aminopyridine shows η^1 coordination through N atom of the pyridine ring (N1). The bridging coordination of the carboxylate oxygen atoms results in the formation of an eight-membered puckered ring ($Cu_2O_4C_2$) motif to construct the overall structure (Fig. 1c). The Cu—Cu distance within the eight-membered ring is 5.268 Å with a O—Cu—O angle of 81.1(11)°.Overall, the coordination number of each of the two Cu^{II} ions in **1**is five and Cu^{II} ions are surrounded by an identical coordination environment (three oxygen atoms and two nitrogen atoms) with a square pyramidal geometry. The Cu(II) ions are perfectly situated in the square plane. Two oxygen atoms of a deprotonated pyridine-2,6-dicarboxylate ligand as well as another carboxylate oxygen atom of a different deprotonated pyridine-2,6-dicarboxylate ligand coordinate meridionally to the central Cu(II) ion. Three corners of the square plane are occupied by the pyridine nitrogen N(3), carboxylate oxygen O(2) and O(3) atoms while the remaining one is occupied by a N(1) atom of the 2-aminopyridine ligand (Fig. 1a). The symmetry generated oxygen atoms O(2) are situated at the apex of the square pyramidal structure (Fig. 1b). The equatorial Cu—O distances (1.992(3) Å, 2.013(3) Å) in **1** are shorter than the axial Cu—O distance (2.739(4) Å) which is expected due to Jahn-Teller effect. It is important to note that the Cu1—N3 bond (1.906(3) Å) is shorter than Cu1—N1 bond (1.983(3) Å) due to the geometrical constraints of the pyridine-2,6-dicarboxylate ligand.

A few further comments on the molecular structure of **1** seem inevitable. Complex **1** displays strong intramolecular N—H···O hydrogen-bonding interactions (Table 3) between the coordinated carboxylate oxygen atom and the non-coordinated $-NH_2$ group of 2-aminopyridine ligand (Table 3). A comprehensive analysis of the crystal structure of **1** reveals the existence of intermolecular hydrogen bonding in the solid state directing to the arrangement of extended 2D chains (Fig. 2). Three non-coordinated water molecules are present in the asymmetric unit and all are involved in

Table 3
Details of hydrogen bond distances (Å) and angles (°) for **1**.

D H···A	d(D H)	d(H···A)	d(D···A)	<(DHA)
N2 – H5 .. O3	0.93(4)	1.91(5)	2.758(5)	151(4)
O5 – H10 .. O4	0.81(8)	2.06(8)	2.865(7)	172(8)
O5 – H11 .. O6	0.80(6)	2.00(6)	2.801(8)	175(8)
O6 – H12 .. O4	0.80(6)	2.07(7)	2.850(6)	163(8)
O6 – H13 .. O7	0.82(8)	1.95(8)	2.758(7)	168(7)
O7 – H14 .. O5	0.80(6)	2.07(6)	2.807(6)	152(6)
O7 – H15 .. O2	0.80(5)	2.11(3)	2.889(5)	164(8)

D, donor; H, hydrogen; A, acceptor.

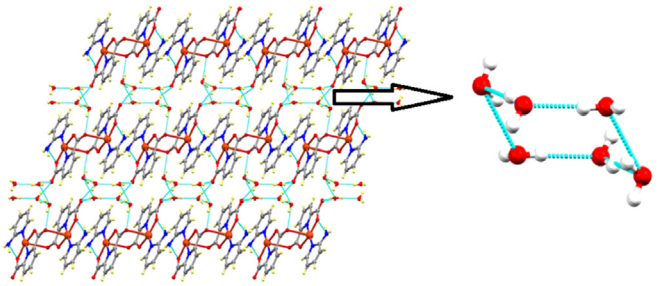

Fig. 2. 2D architecture of H bonding interaction in **1**.

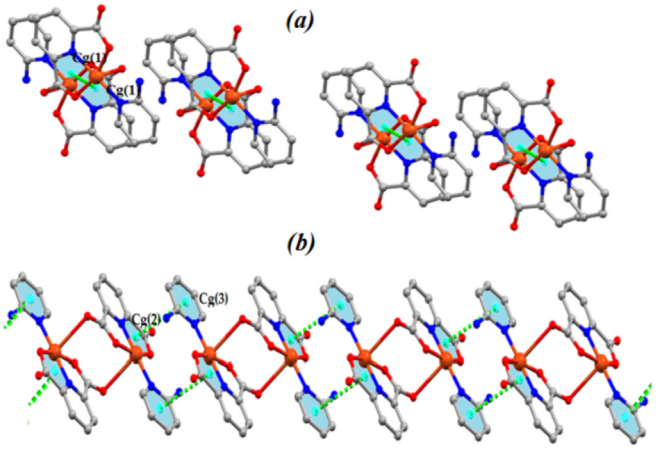

Fig. 3. 1D supramolecular chain generated through π … π interactions (H_2O molecules and H atoms are omitted for clarity).

constructing a $(H_2O)_6$ cluster with chair conformation like cyclohexane. The supramolecular structure of **1** also reveals a 2D architecture, in which a chair conformation of $(H_2O)_6$ clusters are stabilized by hydrogen-bonding interactions with both coordinated and non coordinated O atoms of the carboxylate group (Fig. 2).

In the crystal structure of water hexamer, each water molecule interacts with adjacent water molecules through two hydrogen bonds, one involving one of the two hydrogens and other through oxygen atom by accepting hydrogen bond and thus completing the six-membered ring. The secondhydrogen atom of each water molecule is hydrogen-bonded to the carboxylgroup of dicarboxylic acid. Therefore, water hexamer is bonded to host lattice through 12 hydrogen bonds. In water hexamer structure, O(5), O (5_a), O (6), O (6_a), O (7), O (7_a) act as both hydrogen bond acceptors and donor.

Interestingly, the average O···O distance of 2.759 Å in water hexamer of Complex **1** is closer to the respective distance of ice (2.76 Å for ice I_h at 90 K) than to that of bulk liquid water (2.85 Å). Also, the average O—O—O bond angle of 107.96° is close to the tetrahedral angle in ice I_h form [32,33].

3.2. Non-covalent interactions

Apart from H-bonding, the complex **1** exhibits diverse kinds of weak interactions like π … π, lp … π and N—H … π in solid state structure. These interactions contribute to the self assembly process. Two π … π interactions are responsible to build up supramolecular 1D chain interactions (Fig. 3 and Table 4). Firstly, the 5-membered chelate ring Cu1—O1—C1—C2—N3 (Cg(1)) is stacked over the same chelate ring of an adjacent molecule of symmetry 1-X,-Y,1-Z(3.456 Å). Secondly, the aromatic ring N1—C8—C9—C10—C11—C12 of 2-aminopyridine (Cg(3)) is stacked over the adjacent 5-membered chelate ring Cu1—O3—C7—C6—N3 (Cg(2)) of symmetry 1-X,1-Y,1-Z (3.532 Å). The significant lp … π noncovalent interaction is present in solid state packing of compound **1** (Fig. 4). This lp … π interaction is formed between the non-coordinating carboxylate oxygen atom (O4) and the aromatic ring of 2-aminopyridine Cg(3) (N1—C8—C9—C10—C11—C12) to make 1D crystalline supramolecular building (Table 5). Distance between O4 and Cg(3) is very short (3.594 Å) which signifies a strong lp … π interaction. Another type of N—H … π interaction is present in **1** (between non-coordinating N2—H4 group and chelate ring Cg(1) defined by Cu1—O1—C1—C2—N3) to form 1D supramolecular array with closest distance of 2.95(5) Å (Fig. 5) (Table 6).

3.3. Electrical conductivity measurement

The I—V characteristics within the range from −1 to +1 V for the deposited film shown almost linear and perfectly symmetric nature (Fig. 6). After thermal annealed at 60 °C for 30 min the linear feature of the film become more prominent but current level remains almost same which prove the conductivity is responsible only due to bulk of the compound only, not for contact bias. No improvement was detected even after continuation of the mild annealing process which again supports the conductivity of coordination complex [34,35]. The current level increases from 230 μA to 240 μA after the annealing processes for 30 min. These values are relatively better than those values in other metal based coordination complexes [35]. Furthermore the I—V characteristics of thin film of the compound under dark and illumination of solar light with intensity 100 mW cm^{-2} are presented in the inset. Both two

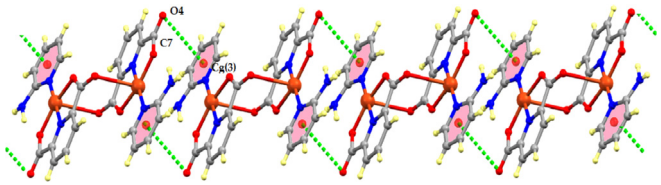

Fig. 4. 1D supramolecular chain generated through lone pair … π interactions (H_2O molecules and H atoms are omitted for clarity).

Table 4
Geometric features (distances in Å and angles in degrees) of the π…π interactions obtained for **Complex 1**.

Complex	Cg(Ring I)…Cg(Ring J)	Cg…Cg	Cg(I)…Perp	Cg(J)…Perp	α	β	γ	Symmetry
Complex 1	Cg1…Cg1	3.456(2)	2.898	2.898	0.00	33.01	33.01	1-X,-Y,1-Z
	Cg2…Cg3	3.532(2)	3.111	3.288	7.22	21.41	28.25	1-X,1-Y,1-Z

α = Dihedral angle between ring I and ring J (°); β = Cg(I)–>Cg(J) or Cg(I)–>Me vector and normal to plane I (°); γ = Cg(I)–>Cg(J) vector and normal to plane J (°); Cg-Cg = Distance between ring Centroids (Å); CgI——Perp = Perpendicular distance of Cg(I) on ring J (Å); CgJ——Perp = Perpendicular distance of Cg(J) on ring I (Å); Cg(1) = centre of gravity of ring [Cu(1)- O(1)-C(1)-C(2)-N(3)]; Cg(2) = centre of gravity of ring [Cu(1)-O(3)-C(7)-C(6)-N(3)] and Cg(3) = centre of gravity of ring [N(1)-C(8)-C(9)-C(10)-C(11)-C(12)].

Table 5
Geometric features (distances in Å and angles in degrees) of the lone pair…π interaction obtained for **Complex 1**.

Complex	C–H…Cg(Ring)	H…Cg (Å)	C–H…Cg (°)	C…Cg (Å)	Symmetry
Complex 1	C7–O4…Cg3	3.594(4)	68.2(3)	3.338(5)	1-X,1-Y,1-Z

For complex 1, Cg(3) = centre of gravity of ring [N(1)-C(8)-C(9)-C(10)-C(11)-C(12)].

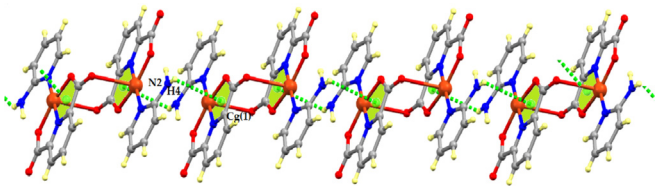

Fig. 5. 1D supramolecular chain generated through NH … π interactions (H_2O molecules and H atoms are omitted for clarity).

curves give ohmic conduction within bias voltage −1 to +1 V. The current changes from 240 μA to 254 μA after illumination of light, giving photosensitivity of 2% (ratio of photocurrent to dark current).

3.4. Geometry optimization and electronic structure

The optimized geometry of dinuclear copper(II) based complex **1** is comparable with molecular structure from SCXRD in Fig. 7 In case of complex **1** in the ground state, the electron density resides mainly on HOMO-1, HOMO-2, LUMO+1 and LUMO+2 orbital occurs at the pyridine-2,6-dicarboxylic acid moiety and 2-aminopyridine ring whereas the electron density on LUMO, HOMO and HOMO−1 orbital remains at 2-aminopyridine ring along with considerable contribution from the d orbital from Cu(II) centre along with an energy gap between HOMO and LUMO of 5.009 eV (Fig. 7).

The UV–Vis absorption spectrum of the complex was studied at room temperature in DMF. The complex shows a well resolved peak at 267 nm and is having MLCT/ILCT character. The band is assigned to $S_0 \rightarrow S_{17}$ electronic transition with excitation energy (5.3686 eV) and oscillator strengths $f = 0.15657$ (Fig. 8).

4. Conclusion

In summary, a new coordination compound [Cu(pydc)(apy)]·$3H_2O$ (**1**) (where $pydcH_2$ = pyridine-2,6-dicarboxylic acid; apy = 2-aminopyridine) is reported. Various non-covalent interactions, like H-bonding, lone pair … π, NH … π and π … π interactions play important roles in the building of an extended network in the synthesized metal-complex framework. It is noteworthy to state that three non-coordinated water molecules participate in constructing a $(H_2O)_6$ cluster in chair conformation of cyclohexane with a centro-symmetrically related group. Knowledge obtained from the above study may also assist to examine various biological processes such as role of water molecules inside channels and or the function of ordered water molecules in biological systems. Electrical conductivity measurement on thin film prepared on glass surface represents the conduction as ohmic and we may conclude that the measured electrical conductivity is responsible only for coordination of complex at ambient temperature. Thus the metal ion of compounds gives high significance in conductivity ground of coordination compounds. Important features of this coordination compound related to biological studies and magnetic properties remain to be investigated further at our end. In our complex **1**, the chair conformation of $(H_2O)_6$ clusters are stabilized by additional hydrogen-bonding interactions with both coordinated and non coordinated O-atoms of the carboxylate group. Thus the strength of H-bonding interaction in complex **1** is much larger than that of Ice

Table 6
Geometric features (distances in Å and angles in degrees) of the NH…π interaction obtained for **Complex 1**.

Complex	C–H…Cg(Ring)	H…Cg (Å)	C–H…Cg (°)	C…Cg (Å)	Symmetry
Complex 1	N2–H4…Cg1	2.95(5)	102(3)	2.816	1-X,1-Y,1-Z

For complex 1, Cg(1) = centre of gravity of ring [Cu(1)-O(1)-C(1)-C(2)-N(3)].

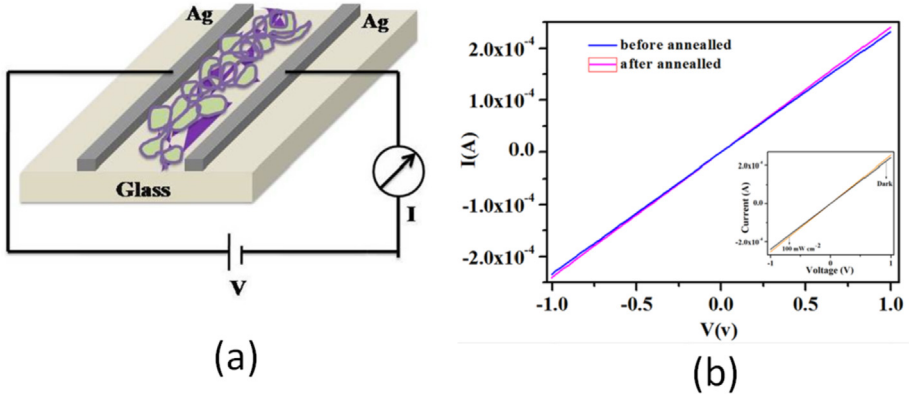

Fig. 6. (a) Schematic diagram of the device for measurement of electron transport, (b) Current – Voltage characteristics of the film before and after annealed realized with the compound. Photo-response in dark and illumination of intensity 100 $mWcm^{-2}$ has shown in inset.

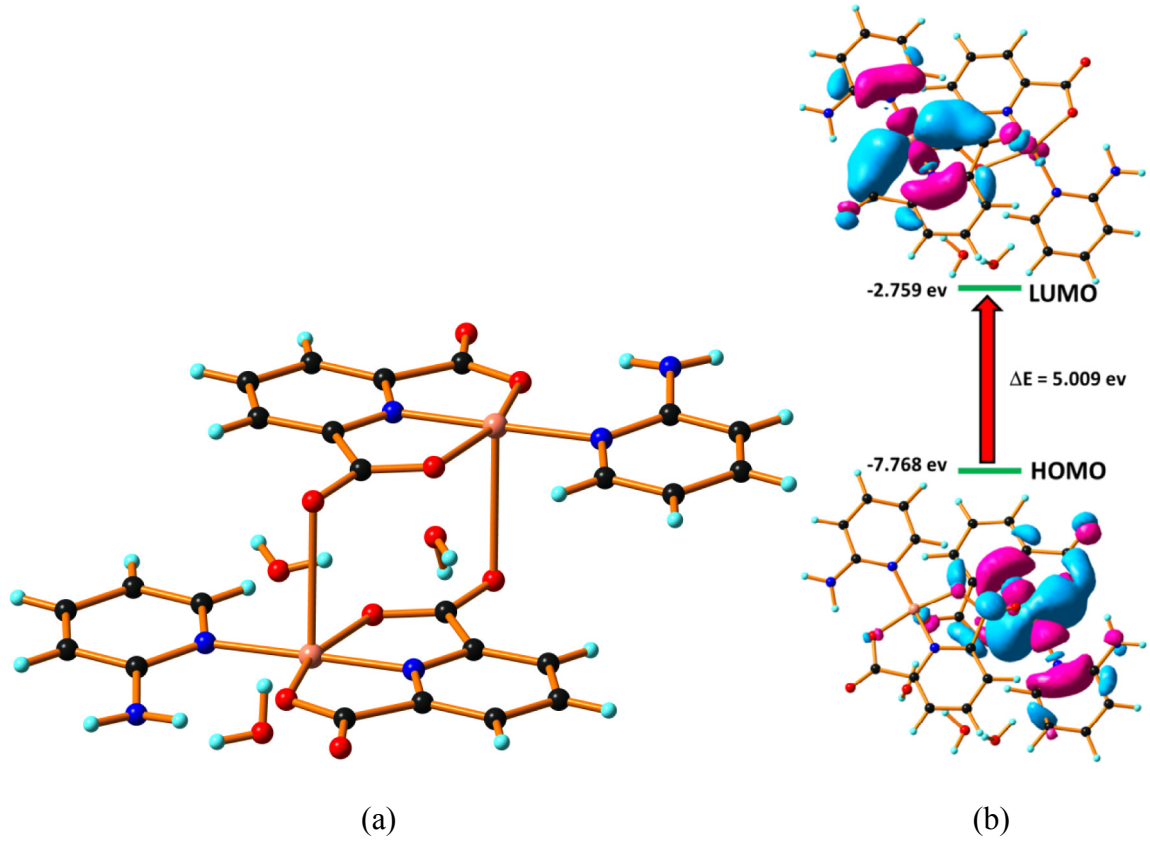

Fig. 7. (a) Optimized geometry and (b) frontier molecular orbitals of complex **1**.

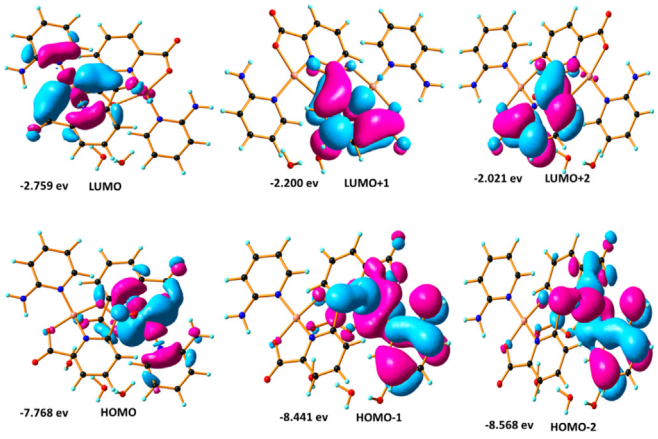

Fig. 8. Frontier molecular orbitals involved in the UV–Vis absorption of the complex **1**.

(I_h) structure. For better understanding of the electronic transitions and the nature of HOMO-LUMO distributions TDDFT (Time Dependent Density Functional Theory) calculations have been carried out on the DFT optimized geometries.

Author contribution

Samit Pramanik - Funding acquisition, Methodology. Saugata Konar - Investigation, Writing - original draft. Koushik Chakraborty – Formal analysis. Tanusri Pal - Visualization. Sourav Das – Data curation. Sudipta Chatterjee – Data curation. Malay Dolai – Software. Sudipta Pathak - Writing - review & editing.

CRediT authorship contribution statement

Saugata Konar: Writing - review & editing. **Sudipta Pathak:** Writing - review & editing.

Acknowledgements

The author Samit Pramanik thanks Council of Scientific and Industrial Research (CSIR, File no. 09/096(0947)/2018-EMR-I), New Delhi, for financial assistance. S. K. is thankful to The Bhawanipur Education Society College, Kolkata 700020 for providing research grant. S. P. is grateful to Haldia Government College, Haldia, Purba Medinipur, 721657 for providing laboratory instrument.

Appendix A. Supplementary data

CCDC 1531475 contains the supplementary crystallographic data for **1**. These data can be obtained free of charge *via* http://www.ccdc.cam.ac.uk/conts/retrieving.html, or from the Cambridge Crystallographic Data Centre, 12 Union Road, Cambridge CB2 1EZ, UK; fax: (+44) 1223-336-033; or e-mail: deposit@ccdc.cam.ac.uk.

References

[1] S. Konar, Inorg. Chem. Commun. 49 (2014) 76–78.
[2] J. Lee, O.K. Farha, J. Roberts, K.A. Scheidt, S.T. Nguyen, J.T. Hupp, Chem. Soc. Rev. 38 (2009) 1450–1459.
[3] M.Y. Masoomi, A. Morsali, Coord. Chem. Rev. 256 (2012) 2921–2943.
[4] J.R. Li, J. Sculley, H.C. Zhou, Chem. Rev. 112 (2012) 869–932.
[5] A.C. McKinlay, R.E. Morris, P. Horcajada, G. Ferey, R. Gref, P. Couvreur, C. Serre, Angew. Chem. Int. Ed. 49 (2010) 6260–6266.
[6] Y. Li, S.S. Zhang, D.T. Song, Angew. Chem. Int. Ed. 125 (2013) 738–741.

[7] S. Konar, J. Mol. Struct. 1092 (2015) 34–43.
[8] A.J. Blake, N.R. Champness, P. Hubberstey, W.S. Li, M.A. Withersby, M. Schro'der, Coord. Chem. Rev. 183 (1999) 117–138.
[9] B. Moulton, M.J. Zaworotko, Chem. Rev. 101 (2001) 1629–1658.
[10] P. Bhowmik, S. Jana, P.P. Jana, K. Harms, S. Chattopadhyay, Inorg. Chim. Acta 390 (2012) 53–60.
[11] B. Li, X. Sun, Inorg. Chem. Commun. 73 (2016) 157–160.
[12] F. Semerci, O.Z. Yeşilel, F. Yüksel, O. Şahin, Inorg. Chem. Commun. 62 (2015) 29–33.
[13] D.L. Boger, J. Hong, M. Hikota, M. Ishida, J. Am. Chem. Soc. 121 (1999) 2471–2477.
[14] H.E. Hosseini, M. Mirzaei, N. Alfi, Review on Proton Transfer Metal Complexes, first ed., Lambert Academic Publishing GmbH & Co. KG, 2012.
[15] S. Khan, S.A.A. Nami, K.S. Siddiqi, E. Husain, I. Naseem, Spectrochim. Acta A. 72 (2009) 421–428.
[16] D.C. Crans, L. Yang, T. Jakusch, T. Kiss, Inorg. Chem. 39 (2000) 4409–4416.
[17] M. Bazargan, M. Mirzaei, H. Eshtiagh-Hosseini, J.T. Mague, A. Bauzá, A. Frontera, Inorg. Chim. Acta 449 (2016) 44–51.
[18] Q. Zang, G.-Q. Zhong, M.-L. Wang, Polyhedron 100 (2015) 223–230.
[19] S.-S. Jew, B.-S. Park, D.-Y. Lim, M.G. Kim, I.K. Chung, J.H. Kim, C.I. Hong, J.-K. Kim, H.-J. Park, J.-H. Lee, H.-G. Park, Bioorg. Med. Chem. Lett 13 (2003) 609–612.
[20] A.C.G. Baró, E.E. Castellano, O.E. Piro, B.S.P. Costa, Polyhedron 24 (2012) 49–55.
[21] F.A. La Porta, J.O.S. Giacoppo, P.H. Ramos, M.C. Guerreiro, T.C. Ramalho, Am. J. Chem. 2 (2012) 255–262.
[22] M. Mirzaei, H.E. Hosseini, Z. Karrabi, K. Molcanov, E. Eydizadeh, J.T. Mague, A. Bauza, A. Frontera, CrystEngComm 16 (2014) 5352–5365.
[23] Bruker, SMART v5.631, Bruker AXS Inc., Madison, WI, USA, 2001.
[24] G.M. Sheldrick, SHELXS-97 and SHELXL-97, University of Göttingen, Göttingen, Germany, 1997.
[25] R. G. Parr and W. Yang, Oxford University Press, Oxford, 1989.
[26] M. Cossi, N. Rega, G. Scalmani, V. Barone, J. Comput. Chem. 24 (2003) 669–681.
[27] A.D. Becke, J. Chem. Phys. 98 (1993) 5648–5652.
[28] W. Lee, W. Yang, R.G. Parr, Phys. Rev. B 37 (1998) 785–789.
[29] R. Bauernschmitt, R. Ahlrichs, Chem. Phys. Lett. 256 (1996) 454–464.
[30] M. J. Frisch, G. W. Trucks, H. B. Schlegel, G. E. Scuseria, M. A. Robb, J. R. Cheeseman, G. Scalmani, V. Barone, B. Mennucci, G. A. Petersson, H. Nakatsuji, M. Caricato, X. Li, H. P. Hratchian, A. F. Izmaylov, J. Bloino, G. Zheng, J. L. Sonnenberg, M. Hada, M. Ehara, K. Toyota, R. Fukuda, J. Hasegawa, M. Ishida, T. Nakajima, Y. Honda, O. Kitao, H. Nakai, T. Vreven, J. A. Montgomery Jr, J. E. Peralta, F. Ogliaro, M. Bearpark, J. J. Heyd, E. Brothers, K. N. Kudin, V. N. Staroverov, R. Kobayashi, J. Normand, K. Raghavachari, A. Rendell, J. C. Burant, S. S. Iyengar, J. Tomasi, M. Cossi, N. Rega, J. M. Millam, M. Klene, J. E. Knox, J. B. Cross, V. Bakken, C. Adamo, J. Jaramillo, R. Gomperts, R. E. Stratmann, O. Yazyev, A. J. Austin, R. Cammi, C. Pomelli, J. W. Ochterski, R. L. Martin, K. Morokuma, V. G. Zakrzewski, G. A. Voth, P. Salvador, J. J. Dannenberg, S. Dapprich, A. D. Daniels, Ö. Farkas, J. B. Foresman, J. V Ortiz, J. Cioslowski and D. J. Fox, Gaussian Inc., 2009, Wallingford CT.
[31] N.M. O'Boyle, A.L. Tenderholt, K.M. Langner, J. Comput. Chem. 29 (2008) 839–845.
[32] D. Eisenberg, W. Kauzmann, The Structure and Properties of Water, Oxford University Press, Oxford, 1969.
[33] N.H. Fletcher, The Chemical Physics of Ice, Cambridge University Press, Cambridge, 1970.
[34] A. Gallego, O. Castillo, C.J.G. García, F. Zamora, S. Delgado, Inorg. Chem. 51 (2012) 718–727.
[35] A. Rana, S.K. Jana, T. Pal, H. Puschmann, E. Zangrando, S. Dalai, J. Solid State Chem. 216 (2014) 49–55.